

2008

## Modulation instabilities in media with relaxational nonlinearities and applications to optical limiting in a photonic bandgap structure

Xue Liu  
*University of Dayton*

Follow this and additional works at: [https://ecommons.udayton.edu/graduate\\_theses](https://ecommons.udayton.edu/graduate_theses)

---

### Recommended Citation

Liu, Xue, "Modulation instabilities in media with relaxational nonlinearities and applications to optical limiting in a photonic bandgap structure" (2008). *Graduate Theses and Dissertations*. 4039.  
[https://ecommons.udayton.edu/graduate\\_theses/4039](https://ecommons.udayton.edu/graduate_theses/4039)

This Thesis is brought to you for free and open access by the Theses and Dissertations at eCommons. It has been accepted for inclusion in Graduate Theses and Dissertations by an authorized administrator of eCommons. For more information, please contact [mschlangen1@udayton.edu](mailto:mschlangen1@udayton.edu), [ecommons@udayton.edu](mailto:ecommons@udayton.edu).

**Modulation Instabilities in Media with Relaxational Nonlinearities and Applications  
to Optical Limiting in a Photonic Bandgap Structure**

Thesis

Submitted To

The School of Engineering of the  
UNIVERSITY OF DAYTON

in Partial Fulfillment of the Requirements for

The Degree

Master of Science in Electro-Optics

By

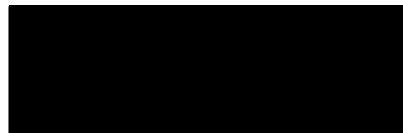
Xue Liu

UNIVERSITY OF DAYTON

Dayton, Ohio

August 2008

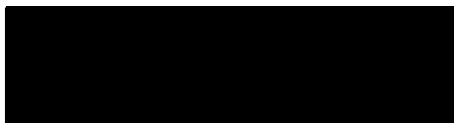
APPROVED BY:



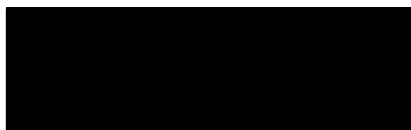
Joseph W. Haus, Ph.D.  
Director and Professor,  
Electro-Optics Program  
University of Dayton  
Committee Chairman




Qiwen Zhan, Ph.D.  
Associate Professor,  
Electro-Optics Program  
University of Dayton  
Committee Member



Peter Powers, Ph.D.  
Associate Professor,  
Electro-Optics Program  
University of Dayton  
Committee Member



Malcolm W. Daniels, Ph.D.  
Associate Dean  
School of Engineering  
University of Dayton



Joseph E. Saliba, Ph.D., P.E.  
Dean,  
School of Engineering  
University of Dayton

## ABSTRACT

Modulation Instabilities in Media with Relaxational Nonlinearities and Applications to  
Optical Limiting in a Photonic Bandgap Structure

Name: Xue Liu  
University of Dayton, 2008

Advisor: Dr. Joseph W. Haus

The advent of lasers created new opportunities to create a wide range of new applications using optical technology. For example, high power lasers are widely used as a tool for industrial, medical and military purposes. Under many circumstances the laser output power can be large enough to cause irreversible damage to the eye or an optical sensor. Thus optical limiting devices have become an outstanding problem that needs to be solved.

In this thesis, we explore a design of a passive optical limiter using one-dimensional photonic bandgap (PBG) structures with embedded materials whose nonlinearity has a temporal response. Firstly, the temporal modulation instability of the non-instantaneous Kerr medium is analyzed by modifying the original nonlinear Schroedinger's equation. The role of the nonlinear response time on reshaping the

solitary wave is examined. Then the spatio-temporal modulation instability of the relaxational Kerr medium is investigated. The gain from modulation instability is derived and its effect on arresting multi-dimensional pulse collapse is studied. Later we numerically investigate counter-propagating beams in a one-dimensional PBG structure with non-instantaneous Kerr nonlinearity. The modulation instability is applied to the design of efficient optical limiters. The performance of the PBG optical limiter with different response times is compared with the instantaneous case. The dynamic range and the cutoff intensity are found to be improved over a range of relaxation times.

## **ACKNOWLEDGEMENTS**

The journey of completing the thesis was full of challenges and difficulties. I would like to thank Dr. Joseph Haus, my advisor, for guiding me the right directions and helping me get over the barriers along the way. I learned from him not only the scientific knowledge and methods, but also the passion in exploring the world of optics. I would also like to thank my committee members, Dr. Powers and Dr. Zhan, for the discussion and advices on my thesis. I'm also very grateful for the help from everyone in the Electro-Optics Department during my graduate studies. Last but not least, I would give special thanks to my family and friends, who have always been there for me and made me the person I am.

## TABLE OF CONTENTS

APPROVAL PAGE.....	ii
ABSTRACT.....	iii
ACKNOWLEDGEMENTS.....	v
TABLE OF CONTENTS.....	vi
LIST OF FIGURES.....	viii
LIST OF TABLE.....	x
CHAPTER	
I. INTRODUCTION.....	1
II. TEMPORAL MODULATION INSTABILITY FOR RELAXATIONAL KERR MEDIUM.....	5
2.1 Analysis of Temporal Modulation Instability for Relaxational Kerr Medium.....	5
2.2 One-Dimensional Solitary Wave Propagation in Relaxational Kerr Medium.....	13
III. SPATIO-TEMPORAL MODULATION INSTABILITY FOR RELAXATIONAL KERR MEDIUM.....	19
3.1 Analysis of Spatio-temporal Modulation Instability for Relaxational Kerr Medium.....	19
3.2 Arresting Multi-Dimensional Pulse collapse in Relaxational Kerr	

Medium.....	25
IV. OPTICAL LIMITING IN A PHOTONIC BANDGAP STRUCTURE WITH RELXATIONAL KERR NONLINEARITY.....	29
4.1 Counter-propagating waves in PBG Structures with Relaxational Nonlinearity.....	29
4.2 PBG Optical Limiter.....	40
V. CONCLUSION.....	45
REFERENCE	



## LIST OF FIGURES

Figure 2-1: Gain spectrum for the instantaneous nonlinear Kerr medium.....	9
Figure 2-2: Gain of the periodic temporal perturbation versus propagation distance. Perturbation parameters: $\varepsilon=0.001$ and $\Omega=2.5$ .....	11
Figure 2-3: The gain spectrum for $\tau_1 = 0.2$ .....	11
Figure 2-4: The gain spectrum for $\tau_2 = 1$ .....	12
Figure 2-5: The gain spectrum for $\tau_3 = 10$ .....	12
Figure 2-6: $\tau = 0.2$ (a) Pulse shape in the medium. (b) N of the medium.....	15
Figure 2-7: $\tau = 1$ (a) Pulse shape in the medium. (b) N of the medium.....	15
Figure 2-8: $\tau = 10$ (a) Pulse shape in the medium. (b) N of the medium.....	16
Figure 2-9: Pulse spreading in non-instantaneous Kerr medium ( $\tau=1$ ) with the initial field $ E_i $ and the final field, $ E_f $ .....	17
Figure 3-1 Spatio-temporal gain spectrum for different types of instantaneous and non- instantaneous ( $\tau = 0.5$ ) Kerr medium.....	23
Figure 3-2 Gain spectrum for self-defocusing, anomalous dispersive noninstantaneous nonlinear medium ( $\tau = 0.5$ ).....	25
Figure 3-3 Spatio-temporal pulse propagating in nonlinear medium	
(a) Initial pulse intensity profile	
(b) Propagated pulse in instantaneous nonlinear medium ( $z=2$ )	
(c) Propagated pulse in fast relaxational nonlinear medium ( $\tau=0.1, z=2$ )	

(d) Propagated pulse in slow relaxational nonlinear medium ( $\tau=1, z=2$ ) .....	26
Figure 4-1. Transmission curve of the PBG structure and the spectrum of the input pulse.....	34
Figure 4-2(a) A snapshot of the pulse evolution through an instantaneous nonlinear medium placed in a PBG.....	35
Figure 4-2(b) A snapshot of the forward- and backward waves with a non-instantaneous nonlinear medium embedded in the PBG. The relaxation time is $\tau_1 = 0.1$ .....	36
Figure 4-2(c) A snapshot of the forward- and backward waves with a non-instantaneous nonlinear medium embedded in the PBG. The relaxation time is $\tau_2 = 1$ .....	36
Figure 4-2(d) A snapshot of the forward- and backward waves with a non-instantaneous nonlinear medium embedded in the PBG. The relaxation time is $\tau_3 = 4$ .....	37
Figure 4-3 3-D structure of the forward propagating pulse.....	39
Figure 4-4 Aperture placed in the Fraunhofer regime to block out energy flow ( $A = 0.75, \tau = 1$ ). The Fresnel number is $F = 10^7$ .....	40
Figure 4-5 Normalized transmissin curve for PBG structures with different response time.....	42

## LIST OF TABLES

Table 4-1 The figures of merit for instantaneous and non-instantaneous nonlinear media embedded in a PBG optical limiter.....	42
---	----

## Chapter I

### Introduction

The rapid advances in lasers have resulted in prevalent applications of laser systems of different power and wavelength in our everyday lives such as compact disc players, supermarket barcode readers and laser pointers. However, the deployment of lasers for military purposes has also been making rapid progress. On the modern battlefield, lasers used as weapons, guidance and detection have increased the potential for accidental or intentional damage to soldiers' eyes and optical systems. The threat to the soldier's well-being and the sensor operation has driven the need for development of eye/sensor protection devices. Miller *et al.* have reviewed the general requirements for optical limiters from the military perspective [1]. Three major requirements must be met for an effective optical limiter. First of all, the device must be effective over a broad wavelength band of the sensor system that is being protected. Secondly, the transmission of the device must be high at the 'off' state and low at the 'on' state. Thirdly, the optical limiter must rapidly respond to the incident optical wave.

During the past years considerable progress has been made in the design of optical limiters. Some of the earliest devices include mechanical or electro-optical shutters. However, there are some severe limitations to their effectiveness. The fastest EO shutter can only respond within  $10\ \mu s$ . While that might be fast enough to prevent damage to a system facing a continuous wave (CW) laser threat, it is too slow when encountering a

short-pulsed laser threat whose temporal width is usually in the order of picoseconds ( $10^{-12} s$ ) or femtoseconds ( $10^{-15} s$ ). The pulse will enter the system unhindered. In both the CW and pulsed cases, however, the optical system is effectively jammed once the shutter is in place. Neutral density filters have also been used to provide limited protection to optical systems by reducing the total amount of light that gets into the system. The disadvantage of this technique is the degradation in performance due to lack of contrast and overall transmission. For some systems, this amount of transmission loss is acceptable or can be compensated for given the alternative of jamming or permanent damage.

Meanwhile, organic materials have shown great promise for optical limiting applications [2]. They possess reverse saturable absorber action where molecules are designed to possess larger excited-state absorption than ground-state absorption. The principal feature is their enhanced nonlinear absorption at higher intensities, but they also possess nonlinear refraction effects [3]. The spectral range of materials can be engineered to cover bands. Of all the organic materials, lead phthalocyanines have absorption bands that can cover the visible and near-IR regimes [4,5].

One dimensional Photonic Band Gap (PBG) structures have been proposed as a fabrication strategy to improve the optical limiting performance of materials. The unusual spatial and temporal dispersion properties of PBGs make them excellent candidates for manipulating the dispersion characteristics of the composite material. This has given rise to a wide range of proposed photonic devices [6-11], among which nonlinear PBG optical limiters have emerged as showing potential due to their compact structure and straightforward fabrication process. The PBG can provide access to the nonlinearity of

materials, such as, metals, that are not normally considered as candidates for optical limiting materials. Scalora et al. recently developed a chirped PBG device with copper layers to induce broadband optical limiting [11]. The chirped dielectric layer thicknesses are designed to improve the linear transmittance and concentrate large fields inside the copper to access the large nonlinearity. An added advantage is that the stack filters the rest of the spectrum outside the visible regime.

PBG optical limiters have been designed by exploiting transverse and longitudinal Modulation Instabilities (MI) using Kerr media [12]. The MI, which has been observed in many nonlinear systems such as plasma physics and fluid dynamics [13-15], refers to the exponential growth of a small perturbation in the medium along propagation. MI has important consequences for optical wave propagation in media with a nonlinear response. Under certain circumstances the MI is closely related to the collapse and break-up of a pulse into sub pulses and broadening of the spectrum. A number of applications has been exploited this phenomenon [16]. MI can also be interpreted as a degenerate four-wave mixing process in the frequency domain. Recent studies show that MI can exist in both self-focusing and self-defocusing medium if the nonlinearity is non-instantaneous [17, 18], which implies new applications in the nonlinear medium.

In this thesis, we concentrate our effort in designing optical limiter using 1-dimensional PBG structure with relaxational nonlinearity by taking advantage of its modulation instability. In Chapter II, we investigate on the influence of a temporally dispersive Kerr effect on the modulation instability and the propagation of solitary-wave pulse. The role of nonlinear response time on reshaping the solitary pulse is examined. In Chapter III, the spatio-temporal modulation instability of the relaxational Kerr medium is

investigated. The gain from modulation instability is derived and its effect on arresting multi-dimensional pulse collapse is studied. In Chapter IV, the counter-propagating waves in one dimensional PBG structure with relaxational nonlinearity are numerically investigated. The role of the spatial and temporal modulation instabilities on reshaping the forward and backward fields as a function of the relaxation time is elucidated. The finite response time of the Kerr effect is taken into consideration in the model. Based on the nonlinear, defocusing effect of the modulation instabilities, an optical limiter is exploited by placing an aperture in the far field behind the PBG structure. The role of nonlinear response time on the performance of optical limiter is examined.

## Chapter II

### Temporal Modulation Instability for a Relaxational Kerr Medium

#### 2.1 Analysis of Temporal Modulation Instability for Relaxational Kerr Medium

Modulation instabilities (MI) have important consequences for optical wave propagation in media with a nonlinear response. The collapse and break-up of a pulse into sub pulses and broadening of the spectrum has been exploited for a number of applications, including white light generation and the frequency comb for metrology [16]. Under the right circumstances the modulation instability (MI) is deeply connected with optical solitons, such as, found for the Nonlinear Schroedinger's Equation (NLSE) [19]. The NLSE's, in different forms, can describe different types of soliton propagation in nonlinear medium. The simplest (1+1)-dimensional NLSE demonstrates that the temporal soliton is a stable entity that the Group Velocity Dispersion (GVD) is balanced by Self-Phase Modulation (SPM) in the nonlinear Kerr medium, meaning that the index of refraction changes with the wave's intensity [20].

The MI has been observed in many nonlinear systems such as plasma physics and fluid dynamics. In the linearized regime, MI refers to the exponential growth of a small perturbation in the medium along propagation, which can break a Continuous Wave into periodic train of soliton-like pulses [21]. Under certain circumstances the MI can be also interpreted as a degenerate four-wave mixing process in the frequency domain. MI was first studied with coherent light beam in one dimensional self-focusing medium [22]. Later research shows that MI is also found in incoherent beams [23]. Recent studies show that MI can exist in both self-focusing and self-defocusing medium if the nonlinearity is



non-instantaneous [17, 18], which implies new applications in the nonlinear medium like  $\text{CS}_2$  [24, 25]. The spatial-temporal MI of counter-propagating waves was also investigated, implying potential applications in optical limiting [26, 27].

In this chapter, we rewrite the original NLSE into two coupled equations by introducing a single temporal relaxing term  $\tau$ . The modified MI is derived from our equations. Using the dynamical model, the modulation instability growth is verified and solitary wave propagation is numerically studied in detail.

The propagation of optical soliton in instantaneous nonlinear medium can be described by the Nonlinear Schroedinger's Equation (NLSE). When perturbations are ignored, the equation takes the form

$$i \frac{\partial E}{\partial z} = \frac{\beta_2}{2} \frac{\partial^2 E}{\partial t^2} - \gamma |E|^2 E \quad (2-1)$$

where  $E=E(t, z)$  describes the electric field envelope in both time and space.  $\beta_2$  is the Group Velocity Dispersion (GVD) parameter, and  $\gamma$  is nonlinear coefficient for Self Phase Modulation (SPM). This equation provides simple insights into the dynamics of optical solitons. The first term on the right of equation stands for the GVD of the pulse, which alone broadens the optical pulse. The second term represents the nonlinear Kerr effect, which can compress the pulse. When the GVD and the SPM effects exactly balance each other, an optical soliton can be generated that travels without shape distortion.

For non-instantaneous, nonlinear media, because of the delay in the response time in such materials, perturbations of the NLSE are added and the dynamical behavior is affected. A soliton-like pulse propagating in a one dimensional, unbounded Kerr medium,

which has a non-instantaneous nonlinear property characterized by the response time  $\tau$ , will undergo shape distortions on a length scale that is determined by the strength of the perturbation. In this paper we expand the NLSE to a set of coupled equations.

$$i \frac{\partial E}{\partial z} = \frac{1}{2} \frac{\partial^2 E}{\partial t^2} + NE \quad (2-2-a)$$

$$\frac{\partial N}{\partial t} = \frac{1}{\tau} (-N + |E|^2) \quad (2-2-b)$$

For the sake of simplicity, the  $\beta_2$  and  $\gamma$  in equation (2-1) are scaled in the new model.  $N=N(t, z)$  represents the nonlinearity of the medium. The medium dynamics is described by a simple relaxational model in Eq. (2-2-b). The parameter  $\tau$  is the medium's response time. The excitation density  $N$  replaces the original NLSE nonlinearity term  $|E|^2$ . The dynamics of  $N$  is related to the local field intensity and the response time of the Kerr medium.

The MI, which exists in many nonlinear systems, refers to the phenomenon that a weak perturbation from the steady-state solution can grow exponentially with propagation distance. In the NLSE case the MI is a result of the interplay between the GVD and the Kerr effect of the medium.

The steady-state solution to Eq. (2-2) for  $E$  possesses the form of a continuous wave

$$E = E_0 e^{i|E_0|z} \quad (2-3)$$

One key question is whether this continuous wave is stable against small perturbations. To testify, we add small perturbations  $e$  to  $E$

$$E_p = (E_0 + e) e^{i|E_0|z} \quad (2-4)$$

The perturbation of  $N$  from its steady-state value is expressed in a linear form as

$$N_p = N_0 + n, \quad (2-5)$$

where  $n$  is the perturbation from  $N_0$ . Note that both  $n$  and  $e$  can be complex.

We begin the stability analysis by substituting Eqs. (2-4) and (2-5) into Eq. (2-2) with the linearized result being:

$$i \frac{\partial e}{\partial z} = \frac{1}{2} \frac{\partial^2 e}{\partial t^2} + n E_0, \quad (2-6-$$

a)

$$i \frac{\partial n}{\partial t} = \frac{1}{\tau} \left( -n + (e + e^*) E_0 \right). \quad (2-6-$$

b)

It's simple to solve Eqs. (2-6) in the frequency domain. Taking the Fourier transform and eliminating the excitation density  $\tilde{n}$ , the fields are expressed in coupled equations as:

$$\left( k + \frac{\Omega^2}{2} - \frac{E_0^2}{1 + i\Omega\tau} \right) e(\Omega) - \frac{E_0^2}{1 + i\Omega\tau} e^*(-\Omega) = 0 \quad (2-7-$$

a)

$$-\frac{E_0^2}{1 + i\Omega\tau} e(\Omega) + \left( -k + \frac{\Omega^2}{2} - \frac{E_0^2}{1 + i\Omega\tau} \right) e^*(-\Omega) = 0 \quad (2-7-$$

b)

The nontrivial solutions for both  $e(\Omega)$  and  $e^*(-\Omega)$ , leads to the following dispersion relation between  $k$  and  $\Omega$ .

$$k = \pm \sqrt{\frac{\Omega^4}{4} - \frac{\Omega^2 E_0^2}{1 + \Omega^2 \tau^2} (1 - i\Omega\tau)} \quad (2-8)$$

The frequency dependent dispersion and gain coefficients are extracted from this result. The gain is determined by the imaginary part of the wave vector  $k$ . For comparison the well-known gain spectrum for the instantaneous nonlinear medium, the dispersion relation between  $k$  and  $\Omega$  is

$$g(\Omega) = \frac{|\Omega| \sqrt{\Omega_c^2 - \Omega^2}}{2} \quad (2-9)$$

where  $\Omega_c = 2 |E_0|$ .

The “gain spectrum” of instantaneous Kerr medium for  $|E_0|=1$  is plotted in Figure 2-1. The actual frequency and wave vector of the perturbation are shifted from the carrier frequency and wave number values  $\omega_0 + \Omega$  and  $\beta_0 + k$ , respectively. The points in Figure 2-1 are the numerical values of the gain calculated by solving the NLSE equation with a small sinusoidal perturbation.

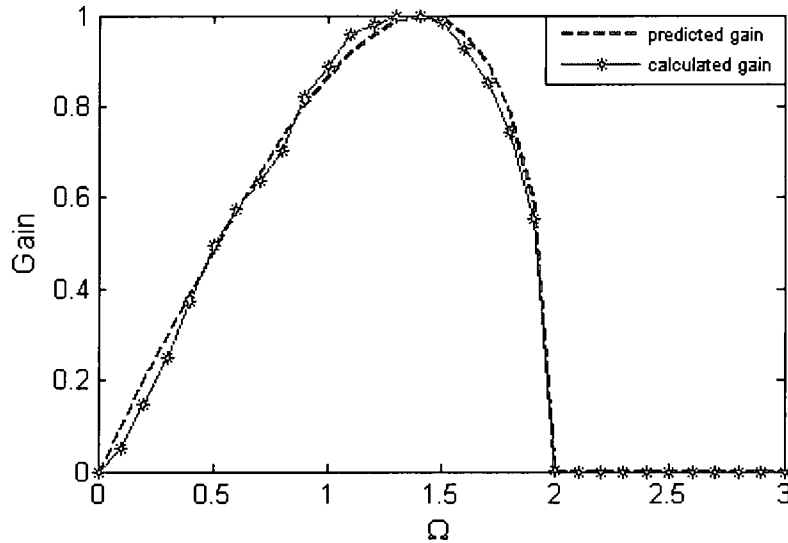


Figure 2-1: Gain spectrum for the instantaneous nonlinear Kerr medium.

As seen in Eq. (2-9) and as illustrated in Figure 2-1, the peak gain occurs when  $\Omega = \frac{\Omega_c}{\sqrt{2}}$  with a value  $g_{\max} = g(\frac{\Omega_c}{\sqrt{2}}) = 1$ . The gain only exists when  $\Omega < \Omega_c$ , indicating that temporally homogeneous wave modulated by noise experiences exponential growth only within the cutoff frequency region. For  $\Omega < \Omega_c$ ,  $k$  is always a real number, meaning that the steady state solution is stable against any perturbation. The gain curve from our simulation agrees with the analytical result.

For non-instantaneous Kerr medium,  $\tau \neq 0$ , the modified NLSE are solved. From Eq. (2-8),  $k$  remains complex in the entire frequency domain. The real part of  $k$  indicates that the wave always propagates with certain periodicity  $Z = \frac{2\pi}{\text{Re}(k)}$ . The imaginary part of  $k$  shows that during propagation, the amplitude of the perturbation increases exponentially with distance. Put into equation,

$$\left| \frac{e(z)}{e(0)} \right| = \exp(g(\Omega)z), g(\Omega) = \text{Im}(k) \quad (2-10)$$

The propagation of a small perturbation in the non-instantaneous nonlinear medium can be interpreted as a combination of periodically repetitive propagation and exponential growth of perturbation amplitude at the same time. We choose sinusoidal perturbation at  $z=0$ , i.e.  $e(t) = \varepsilon \cos(\Omega t)$ , in our numerical experiment, where  $\varepsilon$  is a small parameter and the frequency  $\Omega$  is varied. Figure 2-2 illustrates the growth of a harmonic perturbation in the non-instantaneous nonlinear medium. Three typical relaxational response parameters chosen for further analysis are:  $\tau_1 = 0.2$ ,  $\tau_2 = 1$  and  $\tau_3 = 10$ . By analyzing the variance in the perturbation amplitude with propagation distance, the gain can be extracted. Using different perturbation frequencies the gain “spectra” are calculated.

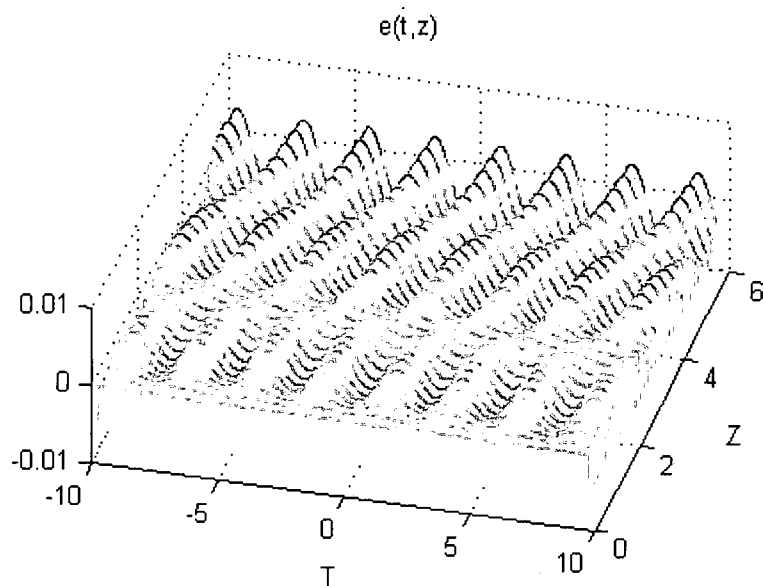


Figure 2-2: Gain of the periodic temporal perturbation versus propagation distance.

Perturbation parameters:  $\varepsilon=0.001$  and  $\Omega=2.5$ .

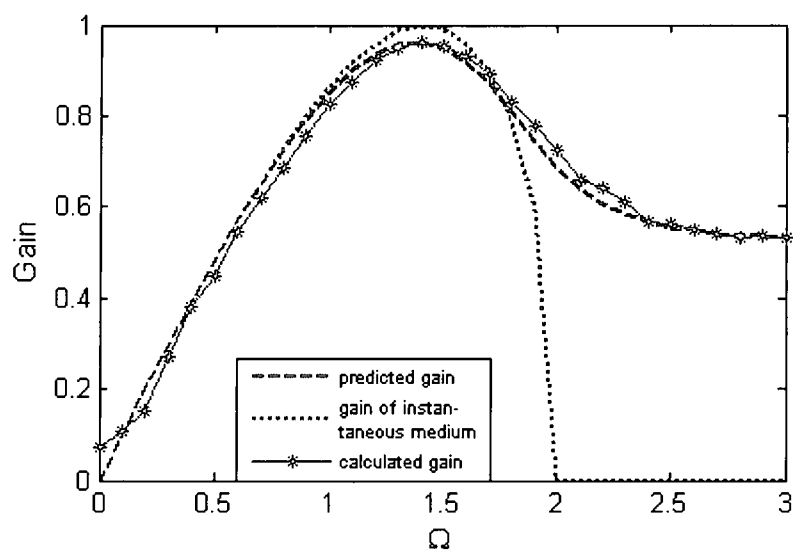


Figure 2-3: The gain spectrum for  $\tau_1 = 0.2$ .

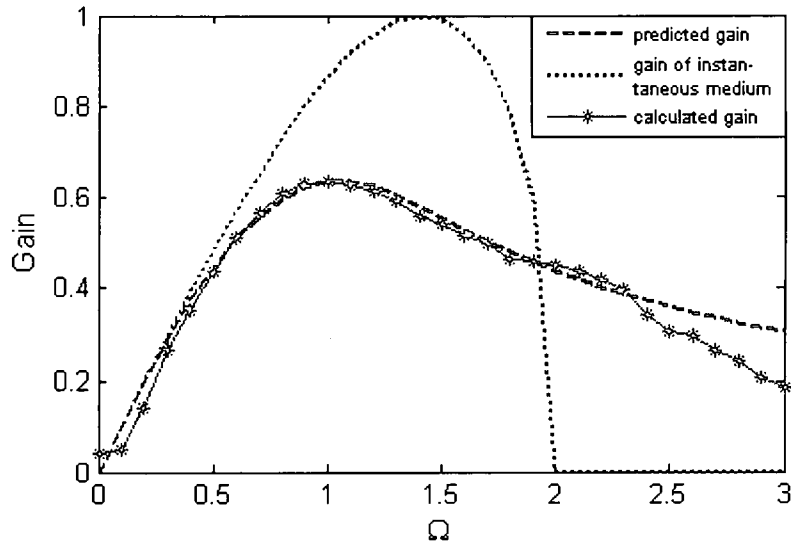


Figure 2-4: The gain spectrum for  $\tau_2 = 1$ .

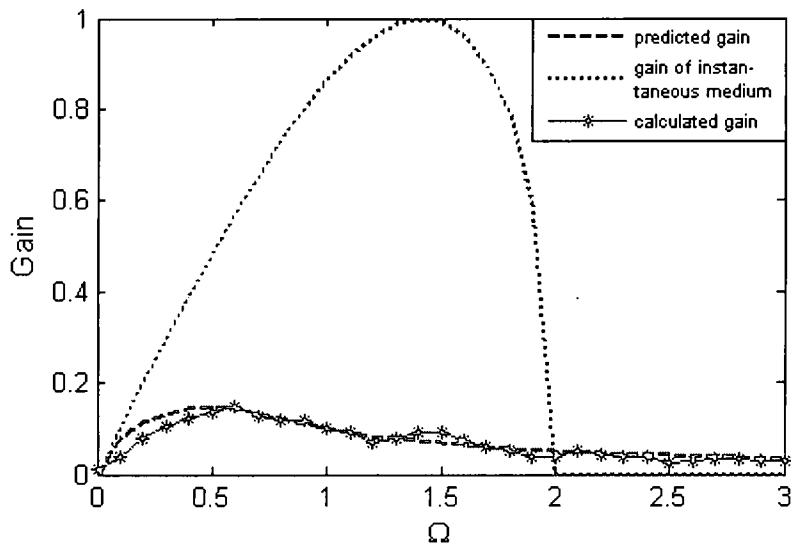


Figure 2-5: The gain spectrum for  $\tau_3 = 10$ .

The graphs of the gain versus frequency in Figure 2-(3-5) demonstrate that there is a broader gain bandwidth for the non-instantaneous nonlinear medium and the peak gain is reduced as the relaxation time increases. There is excellent agreement between the theoretical predicted gain curve and our numerical simulation of the periodic amplitude

gain. Only the positive frequency side of the gain curve is shown here; the spectra are symmetric around  $\Omega=0$ .

As noted the peak gain decreases, as the relaxing time  $\tau$  increases. This can be interpreted by treating the modulation instability as a four-wave mixing process, the perturbation being the probe waves and the CW pump beam. The energy of the two photons from the pump produces two new conjugate frequency photons. For a specific frequency pair  $\pm \Omega$ , the gain coefficient is roughly reduced by the term  $1 + (\Omega\tau)^2$  (see Eq. (2-8)). In the time domain for small relaxation times, a term similar to the Raman contribution is added and the pulse undergoes a redistribution of energy from the pump frequency to lower frequencies. At higher frequencies the gain is reduced because of weaker coupling between the waves.

Comparing the gain curves of the instantaneous nonlinear medium and its counterpart, the gain peak is from  $\pm \Omega_c / \sqrt{2}$  toward the carrier frequency. The reason for this phenomenon is that the relaxing time  $\tau$  depresses the gain at low and intermediate frequencies ( $\Omega < 2$ ). On the other hand the cutoff at  $\Omega = 2$  when  $\tau = 0$  is relaxed because the marginal instability has been replaced by a pair of solutions giving gain and loss and both are excited by a general initial condition.

## **2.2 One-Dimensional Solitary Wave Propagation in Relaxational**

### **Kerr Medium**

With the modified model, the influence of the non-instantaneous Kerr medium on the solitary wave propagation can be studied. One popular numerical method used to solve Eq. (2-2-a) is called the split-step or spectral method [28, 29]. In this method the



linear and nonlinear parts of the partial-differential equation are separated and handled in separate steps. By doing so, we rewrite equation (2-2-a) in the following form

$$\frac{\partial E}{\partial z} = -\frac{i}{2} \frac{\partial^2 E}{\partial t^2} - iNE = [\tilde{D} + \tilde{N}]E \quad (2-11)$$

where  $\tilde{D} = -\frac{i}{2} \frac{\partial^2}{\partial t^2}$  and  $\tilde{N} = -iN$  are the linear and the nonlinear operator respectively.

The linear step of this method can be easily done in the frequency domain and the nonlinear step can be treated in the time domain. Fast Fourier transform methods are applied to solve the dynamical equations. The second-order solution for  $E$  at incremented distance  $z + \Delta z$  is found to be

$$E(t, z + \Delta z) = \exp\left(\frac{\Delta z D}{2}\right) \exp(\Delta z N) \exp\left(\frac{\Delta z D}{2}\right) E(t, z) \quad (2-12)$$

The precision of the numerical solution depends on both the time-frequency domain resolutions and the step sizes along the propagation direction.

The integral form solution of Eq. (2-2-b) is

$$N(t, z) = \frac{1}{\tau} \int_{-\infty}^t e^{-\frac{(t-t')}{\tau}} |E(t', z)|^2 dt' \quad (2-13)$$

Equations (2-12) and (2-13) constitute the mathematical framework for our computer calculations. We examine the effect of non-instantaneous Kerr mediums on the propagation of the soliton-like pulse with a hyperbolic secant intensity profile in time, that is,

$$E(t) = \sec h(t). \quad (2-14)$$

This is the fundamental soliton solution of the instantaneous NLSE.

Again, for our illustration of the perturbation effects, three typical relaxational response parameters are chosen  $\tau_1 = 0.2$ ,  $\tau_2 = 1$  and  $\tau_3 = 10$ .

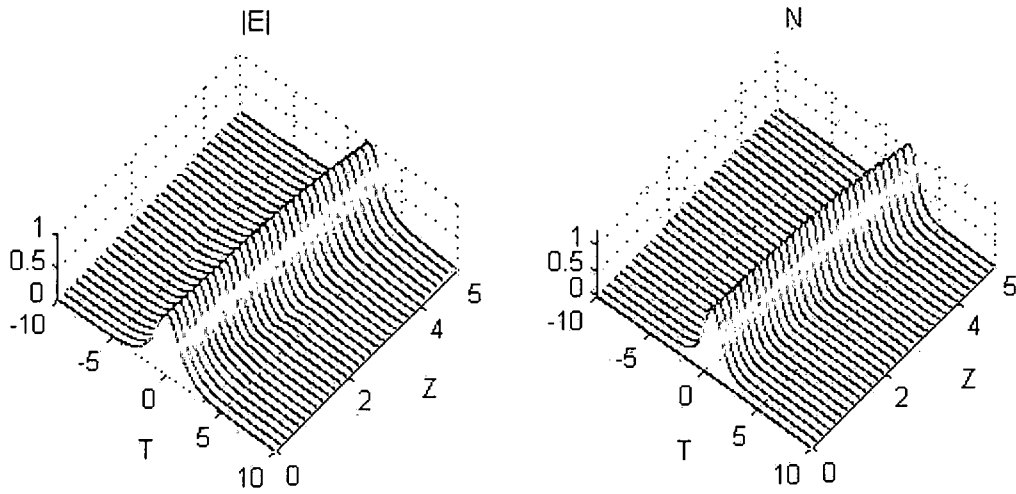


Figure 2-6:  $\tau = 0.2$  (a) Pulse shape in the medium (b)  $N$  of the medium. We follow the propagation to  $z=5$ .

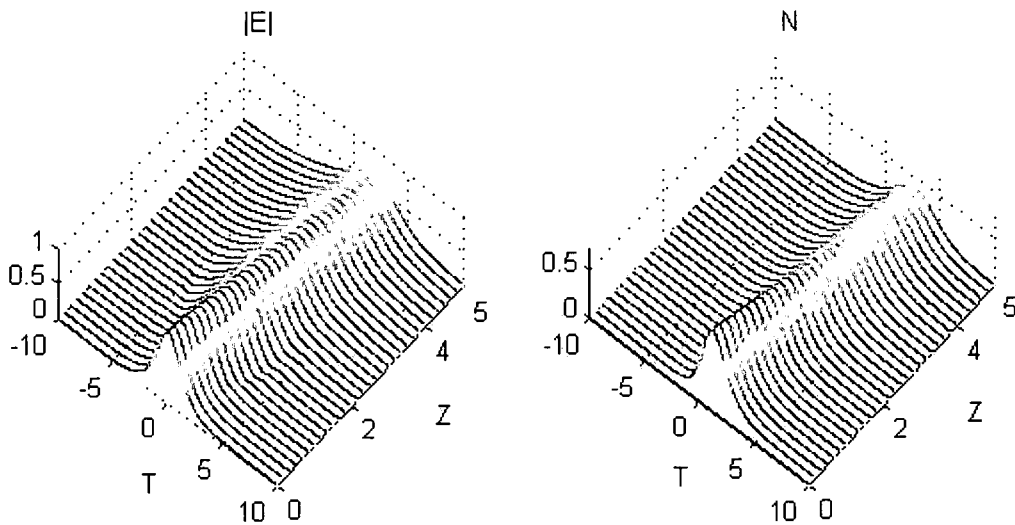


Figure 2-7:  $\tau = 1$  (a) Pulse shape in the medium (b)  $N$  of the medium.

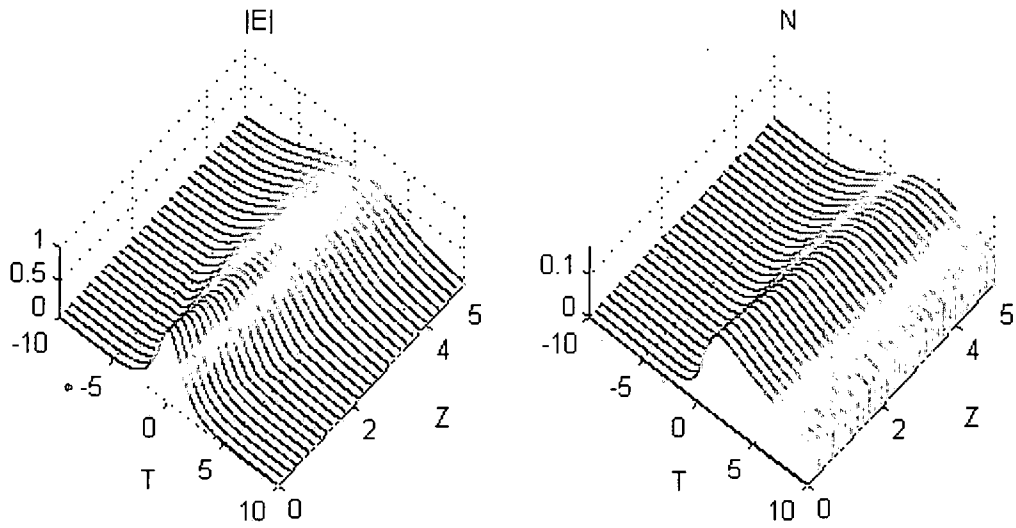


Figure 2-8:  $\tau = 10$  (a) Pulse shape in the medium (b)  $N$  of the medium.

Comparison between Figures (2-6)-(2-8) leads to several observations about the affect of the non-instantaneous nonlinear medium. The graphs of the excitation density  $N$ , show the delayed response that develops in the medium yielding a persistent tail as the pulse passes a given position. The pulse peaks are delayed to longer times and eventually the pulse envelope is severely broadened. Analysis of the pulse spectrum shows that its peak is shifted to higher frequencies. The process is analogous to the red-shifted frequency shift found in intra-pulse stimulated Raman scattering. The pulse delay is more evident for the shorter relaxation times and the effect of a finite relaxation time is already apparent for  $\tau=0.2$ . As  $\tau$  increases, the magnitude of  $N$  decreases, and the effect of the nonlinearity is diminished, which also limits the frequency shift. The balance between the nonlinearity and the dispersion cannot be maintained over distances that are sufficiently long.

This is intuitively understandable because  $\tau$  also determines the magnitude of the nonlinear response in our model. As stated earlier, the optical soliton is a dynamical

entity derived from the balance between GVD and SPM. When the Kerr effect becomes weaker, it no longer balances the dispersion and the pulse spreads. Figure 2-8 shows that for a soliton-like pulse propagating in non-instantaneous Kerr medium ( $\tau=1$ ), after certain distance ( $z=5$ ), the maximum of  $N$  drops to about 40% of that for the instantaneous nonlinear medium. The pulse, unable to maintain its shape broadens in an asymmetric way as shown in Figure 2-9, where the initial and final field envelope pulse profiles are shown. This pulse spreading process, in return, leads to even weaker Kerr effect along the propagation.

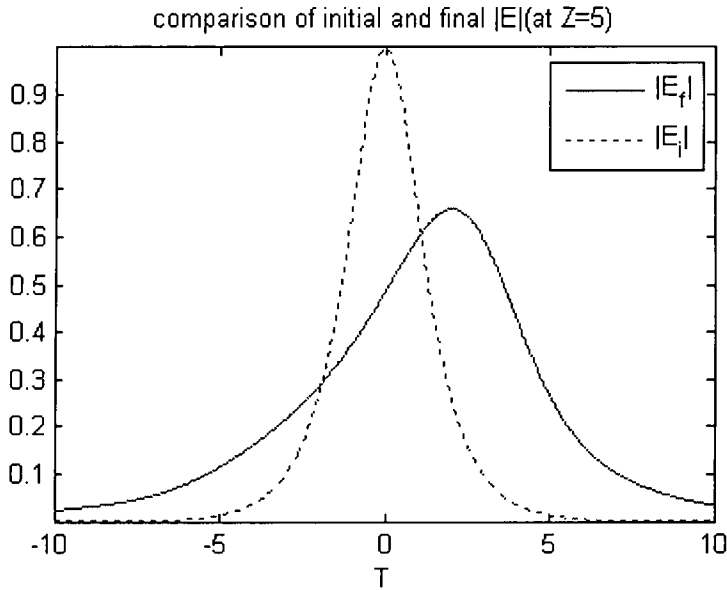


Figure 2-9: Pulse spreading in non-instantaneous Kerr medium ( $\tau=1$ ) with the initial field  $|E_i|$  and the final field,  $|E_f|$ .

To conclude, we presented the effect of non-instantaneous Kerr medium on the MI and showed its affect on the propagation of a soliton-like pulse. We showed that the finite response time of Kerr effect alters the MI by lowering the gain and removing the gain cutoff frequency. It is analytically shown and numerically demonstrated that a long relaxing time of the medium diminishes the nonlinear Kerr effect, resulting in a failure to

maintain the shape of the soliton-like pulse. Compared with the ideal Kerr medium, the new “gain bandwidth” is no longer limited to a frequency region below the cutoff frequency,  $\Omega_c$ . For  $\Omega < \Omega_c$ , the gain decreases because fewer photons are generated by the Four-Wave mixing procedure due to the smaller effective nonlinearity. There is a crossover around  $\Omega_c$  where the tail of the gain curve extends to high frequencies. For  $\Omega > \Omega_c$ , unlike the instantaneous Kerr medium, the MI gain region is extended to break-up temporal pulses at higher frequencies. The soliton-like pulses undergo a frequency shift, similar to that found for stimulated Raman scattering, which delays the pulses to later times.

## Chapter III

### Spatio-temporal Modulation Instability for a Relaxational Kerr Medium

#### 3.1 Analysis of Spatio-temporal Modulation Instability for Relaxational Kerr Medium

Depending on whether the optical beam in the nonlinear medium is modulated by dispersion or diffraction, the modulation instability is classified as temporal [28] or spatial [30, 31] types, respectively. When both of them are present simultaneously, the spatio-temporal instability occurs, e.g., a multi-dimensional pulse propagating in the nonlinear bulk medium is affected by the spatio-temporal modulation instabilities transversely and longitudinally. Previous studies [32-34] of instantaneous nonlinear medium show that for self-focusing medium, the MI occurs for both normal and anomalous dispersion. But for self-defocusing medium, the instability only exists in the normal dispersion regime. Because the modulation instability manifests the breakup of the continuous wave into a train of ultra-short pulses, it is also often treated as a precursor to the generation of optical solitons, such as, found for the (3+1) dimension Nonlinear Schroedinger's Equation (NLSE).[35]

$$i \frac{\partial E}{\partial z} = \frac{\beta_2}{2} \frac{\partial^2 E}{\partial t^2} - \frac{1}{2\beta_0} \left( \frac{\partial^2 E}{\partial x^2} + \frac{\partial^2 E}{\partial y^2} \right) - \gamma |E|^2 E \quad (3-1)$$

$\beta_2$  denotes the Group Velocity Dispersion,  $\beta_0$  is the propagation constant.  $\gamma$  is responsible for the Self-phase Modulation.  $\beta_2$  and  $\gamma$  can be either positive or negative depending on the material property. The pulse propagates along  $z$  direction,  $x$  and  $y$  being the transverse directions. For non-instantaneous nonlinear medium characterized by a

finite response time, the change in the refractive index depends on the time average of the light intensity. Considering that, we rewrite Eq. (3-1) as a set of coupled equations by adding a time-relaxation term.

$$i \frac{\partial E}{\partial z} = \frac{\beta_2}{2} \frac{\partial^2 E}{\partial t^2} - \frac{1}{2\beta_0} \left( \frac{\partial^2 E}{\partial x^2} + \frac{\partial^2 E}{\partial y^2} \right) - \gamma N E \quad (3-2-a)$$

$$\frac{\partial N}{\partial t} = \frac{1}{\tau} (-N + |E|^2) \quad (3-2-b)$$

The parameter  $\tau$  is the medium's response time. Like in Chapter II, the excitation density  $N=N(t, z)$  replacing the  $|E|^2$  term in the original NLSE describes the medium dynamics.  $N$  is related to the local field intensity and the response time of the Kerr medium.

To derive the Spatio-temporal modulation instability of the relaxational nonlinear medium, we follow the same path as in Chapter II. The steady-state solution of Eq. (3-1) has the form of a Continuous Wave (CW) independent of  $x, y$  and  $t$ , which is

$$E(x, y, z, t) = \sqrt{I_0} \exp(i\gamma z) \quad (3-3)$$

Where

$$\gamma = \frac{\beta_0 n_2}{n_0} I_0 = \frac{2\pi}{\lambda} n_2 I_0$$

During propagation, the CW remains unchanged except acquiring an intensity dependent phase shift induced by Self Phase Modulation (SPM). To examine if this CW is stable against small perturbation, we perform a linear stability analysis on equation (3-2) with dynamic perturbation on both  $E$  and  $N$ . Let

$$E_p = (E_0 + e) e^{i|E_0|^2 z}, \quad N_p = N_0 + n$$

Plug in equation (3-2), and the linearized form is

$$i \frac{\partial e}{\partial z} = \frac{\beta_2}{2} \frac{\partial^2 e}{\partial t^2} - \frac{1}{2\beta_0} \left( \frac{\partial^2 e}{\partial x^2} + \frac{\partial^2 e}{\partial y^2} \right) - \gamma n E_0 \quad (3-4-a)$$

$$\frac{\partial n}{\partial t} = \frac{1}{\tau} (-n + (e + e^*) E_0) \quad (3-4-b)$$

Eqs.(3-4) are easier to solve in the frequency domain. By taking the Fourier transform of  $e$  and its complex conjugate, we get

$$\left( k_z + \frac{\beta_2 \Omega^2}{2} - \frac{k_x^2 + k_y^2}{2\beta_0} + \frac{\gamma E_0^2}{1 + i\Omega\tau} \right) e(\Omega, k) + \frac{\gamma E_0^2}{1 + i\Omega\tau} e^*(-\Omega, -k) = 0 \quad (3-5-a)$$

$$\frac{\gamma E_0^2}{1 + i\Omega\tau} e(\Omega, k) + \left( -k_z + \frac{\beta_2 \Omega^2}{2} - \frac{k_x^2 + k_y^2}{2\beta_0} + \frac{\gamma E_0^2}{1 + i\Omega\tau} \right) e^*(-\Omega, -k) = 0 \quad (3-5-b)$$

To get the nontrivial solutions for both  $e(\Omega)$  and  $e^*(-\Omega)$ , the determinant of Eqs.(3-5) must be 0, from which we obtain the dispersion of  $k$ .

$$k_z = \pm \sqrt{\left( \frac{k_x^2}{2} + \frac{k_y^2}{2} - \beta_0 \beta_2 \frac{\Omega^2}{2} \right) \left( \frac{k_x^2}{2} + \frac{k_y^2}{2} - \beta_0 \beta_2 \frac{\Omega^2}{2} - \frac{2\gamma E_0^2}{1 + i\Omega\tau} \right)} \quad (3-6)$$

To make comparison, the well-known dispersion relation of instantaneous nonlinear medium is given as

$$k_z = \pm \sqrt{\left( \frac{k_x^2}{2} + \frac{k_y^2}{2} - \beta_0 \beta_2 \frac{\Omega^2}{2} \right) \left( \frac{k_x^2}{2} + \frac{k_y^2}{2} - \beta_0 \beta_2 \frac{\Omega^2}{2} - 2\gamma E_0^2 \right)} \quad (3-7)$$

Since  $k_x$  and  $k_y$  only exist in the transverse direction, it is useful to introduce a spatial frequency  $\Omega_s$ , as

$$\Omega_s = \left( \frac{k_x^2 + k_y^2}{\beta_0 \beta_2} \right)^{\frac{1}{2}} \quad (3-8)$$

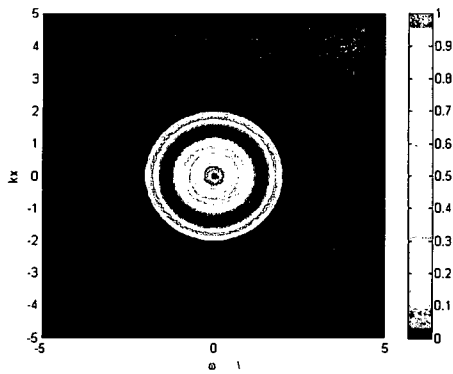
The gain in the energy derived from the dispersion relation is



$$g(\Omega, \Omega_s) = \text{Im}(|\beta_2|^2 \sqrt{(\Omega_s^2 - s_d \Omega^2)(\Omega_s^2 - s_d \Omega^2 - 4s_n \left| \frac{\gamma}{\beta_2} \right| \frac{E_0^2}{1 + i\Omega\tau})}) \quad (3-9)$$

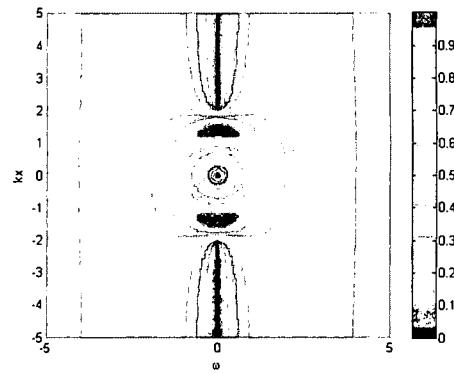
Where  $S_d = \text{sgn}(\beta_2) = \pm 1$ ,  $S_n = \text{sgn}(\gamma) = \pm 1$ .

For different combinations of  $\beta_2$  and  $\gamma$ , the gain patterns varies dramatically, for the sake of comparison, the gain spectrums of both the instantaneous and non-instantaneous mediums ( $\tau = 0.5$ ) are both plotted in Figure 3-1. The horizontal and vertical axes denote the temporal and spatial frequencies, respectively.

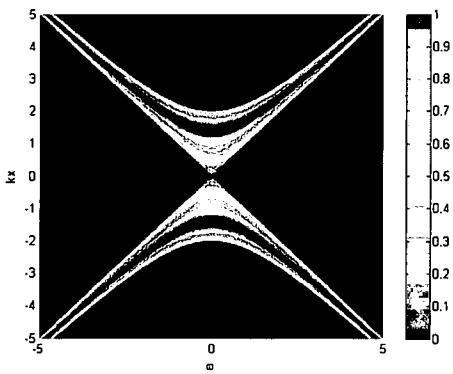


$$s_n = 1, s_d = -1$$

(a) Instantaneous.

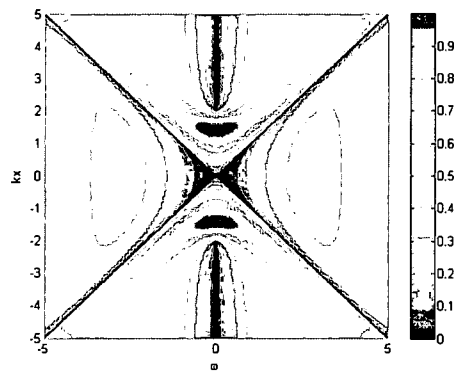


(b) Non-instantaneous.

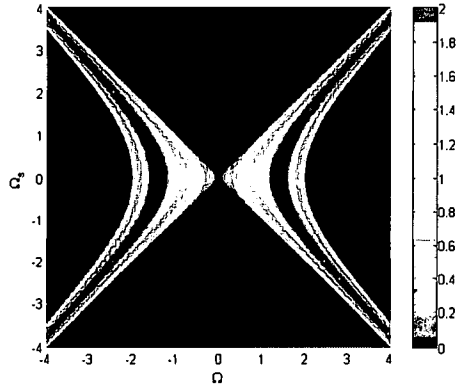


$$s_n = 1, s_d = 1$$

(c) Instantaneous.

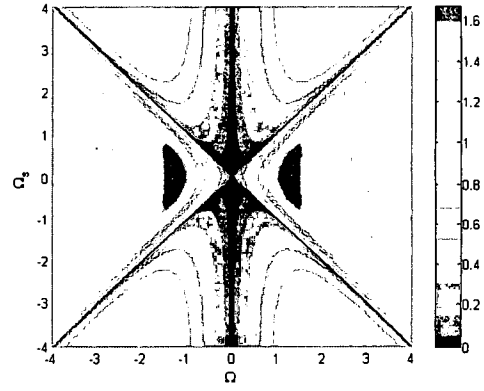


(d) Non-instantaneous.

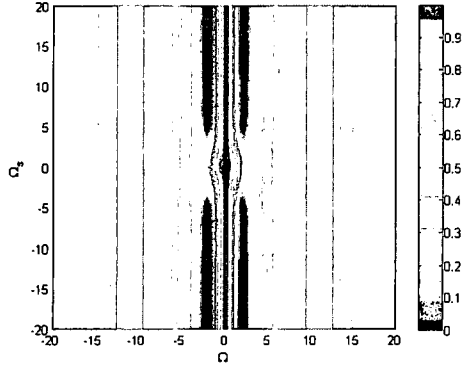


$$s_n = -1, s_d = 1$$

(e) Instantaneous.



(f) Non-instantaneous.



$$s_n = -1, s_d = -1$$

(g) Non-instantaneous.

Figure 3-1 Spatio-temporal gain spectrum for different types of instantaneous and non-instantaneous ( $\tau = 0.5$ ) Kerr medium

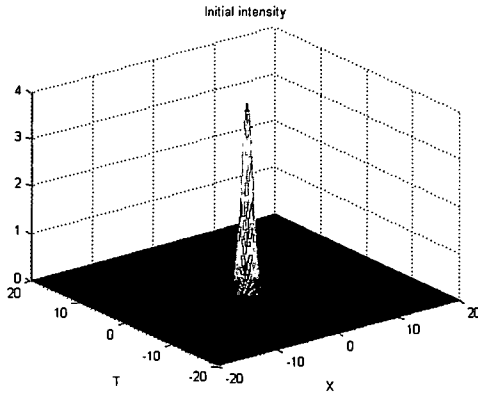
Figure 3-1 (a)(c)(e) show that for the instantaneous nonlinear medium, there are clear borders to limit the existence of gain. However, as seen from figure 3-1 (b)(d)(f)(g), for the non-instantaneous nonlinear medium, the borders of gain are removed and the gain extended to the whole frequency region. This can be explained by eqn.(3-6) in which  $k_z$  stays complex at any frequency to generate gain. We can treat the

MI as a degenerated form of Four Wave Mixing, the perturbation being the probe waves and the CW pump beam. The energy of the two photons from the pump produces two new conjugate frequency photons. In the instantaneous case, to generate MI, phase-match condition is required from the pump and probe, thus the generated frequency is strictly limited. But when the medium response time is taken into account, according to the Debye equation,  $N$  becomes complex, a Raman-like nonlinearity is developed for which self-phase-match is achieved, leading to a gain region outside the original sideband. As stated before, spatial-temporal Modulation Instability comes from the competition between diffraction, dispersion and the second-order nonlinear effect. In the absence of diffraction ( $\Omega_s = 0$ )/dispersion ( $\Omega = 0$ ), the spatial-temporal MI reduces to the temporal/spatial modulation instability.

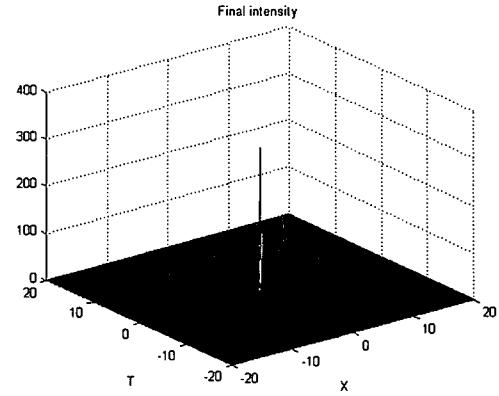
Figure 3-1 shows that the nature of GVD and nonlinearity (the signs of the signs of  $s_n$  and  $s_d$ ) dominantly affect the scope of the gain. Special attention should be given to the medium which is defocusing and anomalously dispersive ( $s_n = -1, s_d = -1$ ). It is acknowledged that the Modulation Instability does not exist if the medium is instantaneously responsive because the nonlinearity and the diffraction work in a similar way of broadening the pulse. However, when the nonlinearity is relaxed by the response time, novel MI starts to occur. As seen from figure 3-2, along the temporal frequency axis, the gain reaches a peak and then relaxes to high frequencies. Meanwhile, along the spatial frequency axis, no peak gain is found, at high frequencies the gain stays almost unchanged. This is a unique property from the other types of nonlinear medium. This phenomenon can be explained as the following: When the optical beam propagates in the self-defocusing medium, the region with lower light intensity shows a higher refractive

reducing of the size of the pulse both spatially and temporally. Ideally, the pulse develops a singularity at a finite propagation distance. Several mechanisms have proved effective in arresting critical collapse, among which there are saturable [39-40] Kerr effect, self-steepening and nonlinear absorption [41].

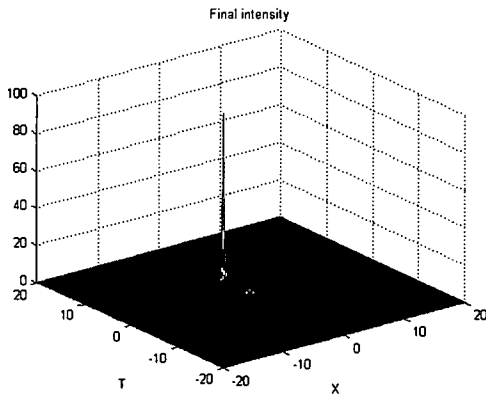
According to the analysis earlier in this chapter, the spatio-temporal gain spectrum is dramatically affected by the nonlinear response time of the medium. To examine the influence of the non-instantaneous nonlinearity on the break-up of the pulse, a 2-dimensional pulse with initial Gaussian profile is launched in mediums with different relaxational times. The final intensity after propagating for a distance  $z=2$  is recorded.



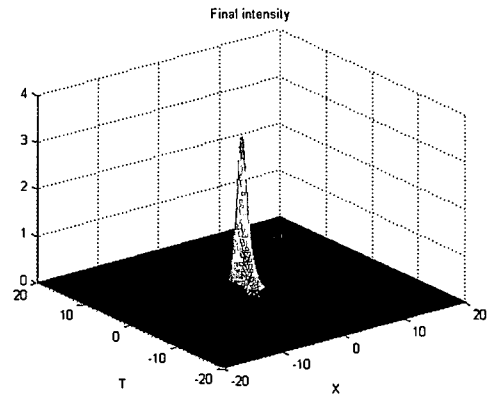
(a)



(b)



(c)



(d)

Figure 3-3 Spatio-temporal pulse propagating in nonlinear medium.

- (a) Initial pulse intensity profile.
- (b) Propagated pulse in instantaneous nonlinear medium ( $z=2$ ).
- (c) Propagated pulse in fast relaxational nonlinear medium ( $\tau=0.1, z=2$ ).
- (d) Propagated pulse in slow relaxational nonlinear medium ( $\tau=1, z=2$ ).

To make comparison, we first show the soliton collapse in the self-focusing and anomalously dispersive instantaneous nonlinear medium in Figure 3-3(b). The collapse threshold for the medium is normalized to 1. The initial intensity of the pulse is set to be 4. After propagating a finite distance of  $z=2$ , the intensity of the pulse rises steeply to more than 300 and the size of the beam shrinks to infinitely small. Ideally, if the pulse continues propagating, a singularity will be formed quickly.

Figure 3-3(c),(d) shows the effect of relaxational nonlinearity on soliton collapse. Unlike in the instantaneous case, in which the index of refraction only increases with intensity (i.e.,  $n = n_0 + n_2 I$ ), the index change in relaxational medium also depends on the relaxation time. Hence the magnitude of excitation density is dominantly affected by  $\tau$ . For short relaxational time  $\tau = 0.1$ , the self-focusing effect is dampened to certain degree, but  $N$  still exceeds the threshold of pulse collapse, the intensity of beam rises nevertheless, the increasing rate is lower than in the instantaneous case. For longer response time like  $\tau = 1$ ,  $N$  decreases below the critical value. The dispersion and diffraction effects become dominant, thus the beam is spread more than converged. The collapse is inhibited to happen. It should be pointed out that because the nonlinearity is only relaxed in the time domain, the collapse is arrested unevenly in time and space,

index. However, due to the delayed response of the medium, if the spatial modulation is moving transversely with a proper frequency, the light of higher intensity can always meet the higher index, similar to the case in which MI occurs in an instantaneous self-focusing medium.

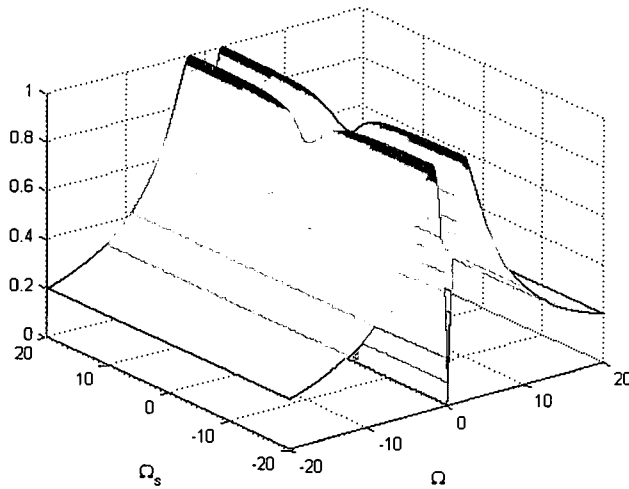


Figure 3-2 Gain spectrum for self-defocusing, anomalous dispersive noninstantaneous nonlinear medium ( $\tau = 0.5$ ).

### **3.2 Arresting Multi-Dimensional Pulse collapse in Relaxational Kerr Medium**

The basic linear analysis for spatio-temporal soliton shows that small fluctuation in the intensity, beam size or pulse width can grow with propagation. In particular, the ultrashort optical pulses in self-focusing and anomalously dispersive type of nonlinear medium have been the subject of intense investigations [36-38]. Previous studies have shown that for the multi-dimensional pulses, categorized as the “1+2” type in a planar waveguide or the “1+3” type in a bulk medium, if the energy exceeds a critical value, the self-focusing effect start to dominate over the diffraction and dispersion, leading to the

leading to the asymmetry of the propagated pulse in such medium as seen from Figure 3-3(d)

## Chapter IV

### Optical Limiting in a Periodic Materials with Relaxational Nonlinearity

#### 4.1 Counter-propagating Waves in PBG Structures with Relaxational nonlinearity

One of the key challenges in the development of optical limiters is the search for appropriate materials that rapidly respond to the applied laser intensity, have good nonlinear absorption characteristics over a broad range of wavelengths and have a high damage threshold. To protect the eyes the transmitted fluence through the device should be clamped under  $500 \text{ nJ/cm}^2$  over a range of visible wavelengths. Dangerous IR radiation could be eliminated by a fixed high pass filter. Organic materials have shown great promise for optical limiting applications. They possess reverse saturable absorber action where molecules are designed to possess larger excited-state absorption than ground-state absorption. The principal feature is their enhanced nonlinear absorption at higher intensities. The spectral range of materials can be engineered to cover bands. Lead phthalocyanines is an outstanding candidate because of its absorption bands in the visible and near- IR regimes [4,5].

One dimensional Photonic Band Gap (PBG) structures have been proposed as a fabrication strategy to improve the optical limiting performance of materials. Earlier work on PBG optical limiters was based on exploiting transverse and longitudinal modulation instabilities using Kerr media [12]. Compared with traditional homogeneous nonlinear optical limiters, this design has shown promising performance for optical limiting, i.e., high transmission for normal light and low for intense beams, effective in



protecting optical elements and sensors against damage by exposure to malicious or unexpected high-intensity light.

In this chapter, the counter-propagating waves in one dimensional PBG structure with relaxational nonlinearity are numerically investigated. The role of the spatial and temporal modulation instabilities on reshaping the forward and backward fields as a function of the relaxation time is elucidated. Again, the finite response time of the Kerr effect is taken into consideration in the model. Based on the nonlinear, defocusing effect of the modulation instabilities, an optical limiter is exploited by placing an aperture in the far field behind the PBG structure. The role of nonlinear response time on the performance of optical limiter is examined.

The dynamical equations for counter-propagating waves in non-instantaneous nonlinear PBG structure can be derived by applying the multiple scales method to the classical nonlinear wave equation [42]. The dynamics of the medium is described by a simple relaxational model with the medium's response time.

$$\frac{1}{v} \frac{\partial E_f}{\partial t} = -\frac{\partial E_f}{\partial z} + \frac{i}{F} \Delta_{\perp}^2 E_f + i\delta E_f + i\kappa E_b + i\eta N_f E_f \quad (4-1-a)$$

$$\frac{1}{v} \frac{\partial E_b}{\partial t} = \frac{\partial E_b}{\partial z} + \frac{i}{F} \Delta_{\perp}^2 E_b + i\delta E_b + i\kappa E_f + i\eta N_b E_b \quad (4-1-b)$$

$$\frac{\partial N_f}{\partial t} = \frac{1}{\tau} (-N_f + |E_f|^2 + 2|E_b|^2) \quad (4-1-c)$$

$$\frac{\partial N_b}{\partial t} = \frac{1}{\tau} (-N_b + |E_b|^2 + 2|E_f|^2) \quad (4-1-d)$$

where the fields  $E_f = E_f(x, z, t)$  and  $E_b = E_b(x, z, t)$  describe the electric field envelope of the forward and backward waves in space and time. We denote by  $x$  the transverse coordinate, since we will treat only a single transverse dimension in our PBG structure;  $v$

denotes group velocity,  $F$  is the Fresnel parameter,  $\delta = k - k_0$  stands for the detuning of the initial pulse wave number from the center of the stop band,  $k_0 = \frac{\pi}{\Lambda}$  where  $\Lambda$  is the lattice constant.  $\kappa$  denotes the coupling coefficient of the grating,  $\eta$  is the nonlinear Kerr coefficient, which is assumed homogeneous throughout the medium. In our numerical model, the index change of the two materials is assumed to be weakly periodic.  $N_f$  and  $N_b$  represent the excitation densities of the nonlinear medium for the forward and backward waves, respectively. The finite response time of Kerr effect of the PBG structure is denoted by  $\tau$ . From Eqs. (4-1-c) and (4-1-d) it is clear that dynamics of  $N$  is not only related to the local field intensities of both waves, but also the response time of the medium.

We consider the case that the signal is only launched into one side of the PBG structure. Therefore, the boundary conditions we applied to the model are

$$E_f(x, 0, t) = E_f(x, t) \quad (4-2-a)$$

$$E_b(x, L, t) = 0 \quad (4-2-$$

b)

In our previous research [43], a novel split-step method has been introduced to solve Eq. (4-1). By separating the propagation into 2x2 matrices, we express Eq. (4-1) in the symbolic matrix form

$$\frac{dU}{dt} = (\tilde{L} + \tilde{N})U \quad , \quad (4-3)$$

where the state vector is

$$U = (E_f, E_b)^T \quad , \quad (4-4)$$

and the operators are

$$\tilde{L} = \begin{pmatrix} -\frac{\partial}{\partial z} + \frac{i}{F}\Delta_{\perp}^2 + i\delta & 0 \\ 0 & -\frac{\partial}{\partial z} + \frac{i}{F}\Delta_{\perp}^2 + i\delta \end{pmatrix} + \begin{pmatrix} 0 & i\kappa \\ i\kappa & 0 \end{pmatrix} = \tilde{V} + \tilde{K} \quad , \quad (4-5-a)$$

$$\tilde{N} = \begin{pmatrix} i\eta N_f & 0 \\ 0 & i\eta N_b \end{pmatrix} \quad . \quad (4-5-b)$$

Matrices  $L$  and  $N$  represent the linear and nonlinear parts of the partial-differential equation are treated differently in separate steps.

For the linear step, because the operator  $L$  can be decomposed to a diagonal and an off-diagonal matrix, we can further simplify the calculations if the step size is small enough. i.e.

$$U_L(t + \frac{dt}{2}) = \exp(\frac{Vdt}{2}) \exp(\frac{Kdt}{2}) U(t) \quad (4-6)$$

where the subscript L stands for the linear propagation contribution. Eq. (4-6) can be readily solved in the Fourier space. In our calculation, 2048 and 1024 points are used for Fast Fourier Transform in the longitudinal and transverse directions, respectively. For the nonlinear step, we first find the analytical solutions for Eqs. (4-1-c) and (4-1-d)

$$N_f(x, z, t) = \frac{1}{\tau} \int_{-\infty}^t e^{-\frac{(t-t')}{\tau}} (2|E_b(x, z, t')|^2 + |E_f(x, z, t')|^2) dt' \quad (4-7-a)$$

$$N_b(x, z, t) = \frac{1}{\tau} \int_{-\infty}^t e^{-\frac{(t-t')}{\tau}} (2|E_f(x, z, t')|^2 + |E_b(x, z, t')|^2) dt' \quad (4-7-b)$$

By assuming that  $N_f$  and  $N_b$  stay constant for a small step size, the solution to the nonlinear step can be written as

$$U_N(t + \frac{dt}{2}) = \exp(Ndt) U(t) \quad (4-8)$$

where the subscript N refers to the nonlinear contribution to the propagation.

Combining the two separated steps together, the second-order solution for  $U$  at the incremented time  $t + dt$  is

$$U(t + dt) = \exp\left(\frac{Vdt}{2}\right) \exp\left(\frac{Kdt}{2}\right) \exp(Ndt) \exp\left(\frac{Vdt}{2}\right) \exp\left(\frac{Kdt}{2}\right) U(t) \quad (4-9)$$

We monitor the accuracy of the numerical method by examining the law of energy conversation at each time step.

The forward propagating pulse is placed outside the PBG structure at certain distance  $z_0$  so that the initial field in the PBG structure vanishes. The intensity distribution of the pulse is in a Gaussian shape transversely and longitudinally, i.e.

$$E_f(x, z, 0) = A \exp(-(z - z_0)^2 / \sigma_z^2) \exp(-x^2 / \sigma_x^2) \quad (4-10)$$

The initial condition for the backward propagating pulse is

$$E_b(x, z, 0) = 0 \quad (4-11)$$

To simplify the calculations, the parameters in Equation 4-1 are scaled as follows:  $\nu = 1, \kappa = 1, \eta = 1$ . We tune the incident laser pulse central angular frequency away from the center of the PBG stop band by changing the value of  $\delta$ . The selection of  $\delta$  is closely related to the spatio-temporal modulation instability of the nonlinear PBG structure, which is essential in influencing the propagation of the pulse. When the first transmission peak of the PBG for positive angular frequency, also called the “band-edge”, overlaps with the center of the pulse spectrum the break-up of the pulse is maximized by the spatio-temporal modulation instability [26]. The transmission curve for the PBG structure used in our simulation with a length  $L=6.1$  is plotted in Figure 4-1. The offset from the center of the pulse spectrum to the band-edge of the PBG is  $\delta = 1.12$ ,

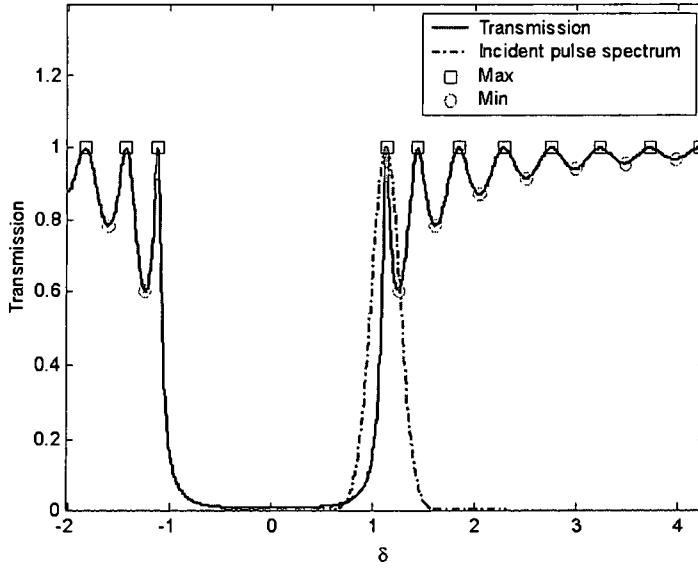


Figure 4-1. Transmission curve of the PBG structure and the spectrum of the input pulse.

Previous papers shows that the threshold of initial amplitude for modulation instability to occur is around  $A=0.3$ . In our simulations, we set the amplitude at  $A=0.75$ , to insure a high modulation instability gain. The different nonlinear response time chosen for the PBG structure are  $\tau_1 = 0.1$ ,  $\tau_2 = 1$  and  $\tau_3 = 4$ . The case for instantaneous PBG structure is also simulated for comparison.

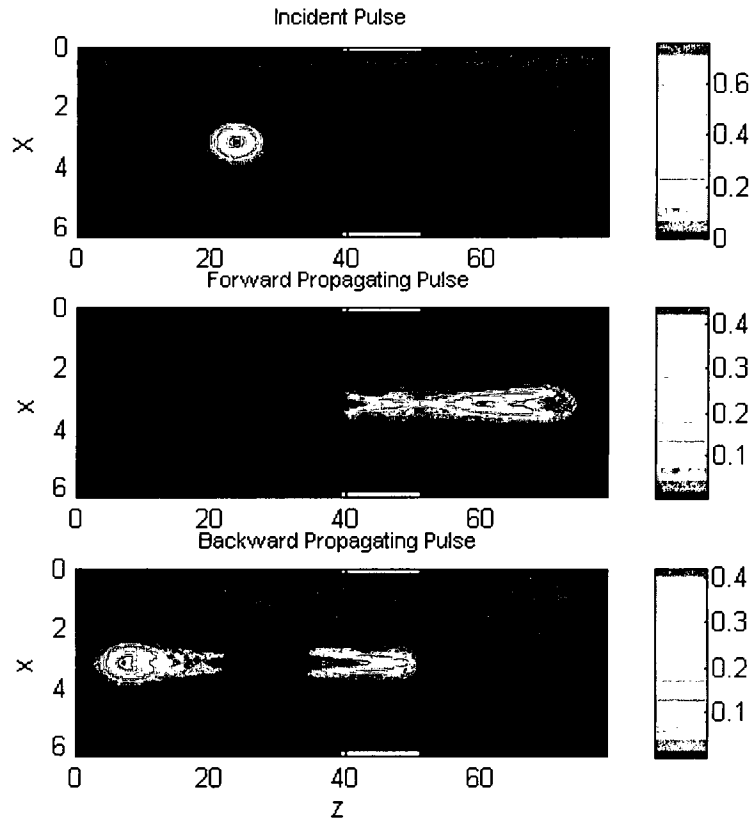


Figure 4-2(a) A snapshot of the pulse evolution through an instantaneous nonlinear medium placed in a PBG. Top frame is the initial pulse, which is launched outside the medium. The central frame and bottom frame are the forward propagating and backward propagating pulse, respectively. The initial amplitude of the wave is  $A=0.75$ .

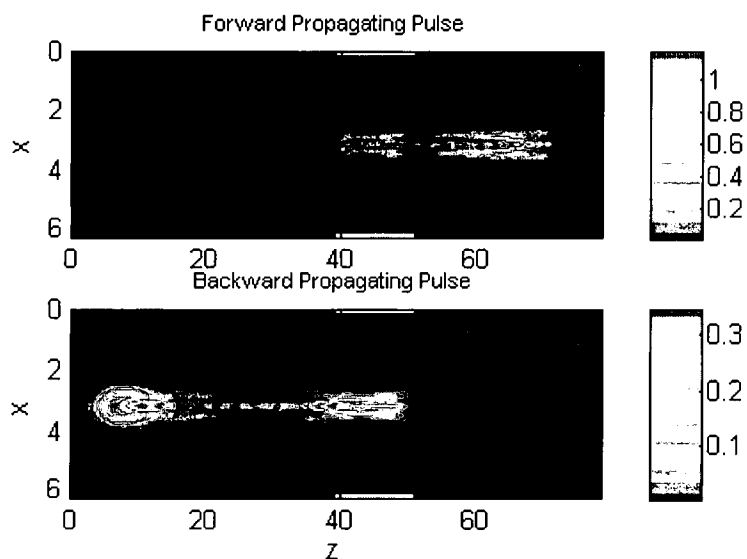


Figure 4-2(b) A snapshot of the forward- and backward waves with a non-instantaneous nonlinear medium embedded in the PBG. The relaxation time is  $\tau_1 = 0.1$  and the amplitude is the same as in Fig. (2a).

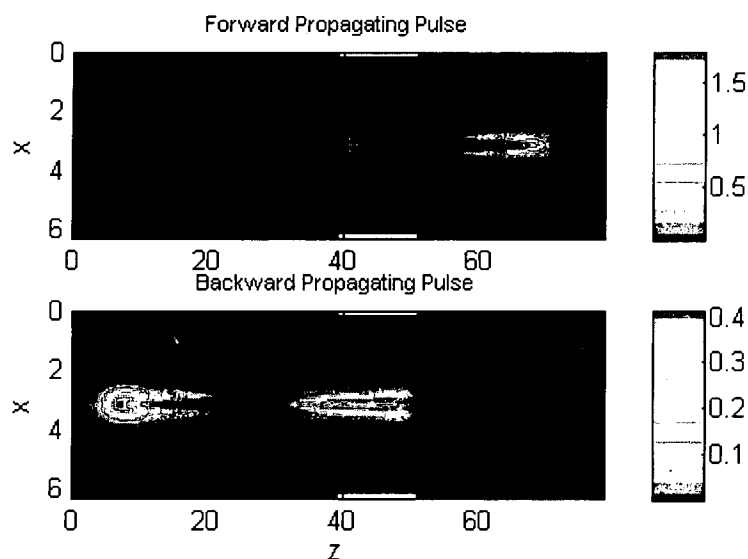


Figure 4-2(c) A snapshot of the forward- and backward waves with a non-instantaneous nonlinear medium embedded in the PBG. The relaxation time is  $\tau_2 = 1$  and the amplitude is the same as in Figure 4-2(a).

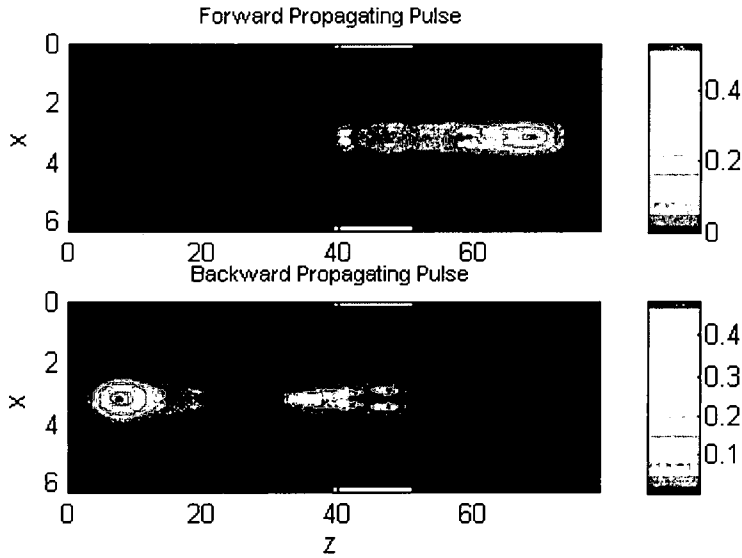


Figure 4-2(d) A snapshot of the forward- and backward waves with a non-instantaneous nonlinear medium embedded in the PBG. The relaxation time is  $\tau_3 = 4$  and the amplitude is the same as in Figure 4-2(a).

Snapshot views of the pulse forward-backward pulse intensities for different relaxation times are shown in Figure 4-2(a)-(d). The position of the PBG medium is denoted by a pair of green bars placed between in the range  $z=(40,50)$ . The absolute amplitude of the field at each pixel is represented by a color with the amplitude shown in the vertical scale on the right side. The vertical axis displays the transverse coordinate and the horizontal axis is the propagation direction.

The top figure is the input Gaussian field; its pulse width is shorter than the medium so that it samples a large portion of the dispersive spectrum in the medium. The middle figure is the continuation of the forward-propagating pulse as it passes into and through the PBG sample. The bottom figure shows the propagation of the backward propagating pulse in the medium. In our computations  $F$  is chosen to be extremely large ( $F = 10^7$ ) so that the transverse coupling is weak and does not noticeably affect the pulse tuning at a



selected frequency. Comparison among Figures 4-2(a) through 4-2(d) leads to several observations about the effect of the non-instantaneous nonlinear PBG structure on pulse propagation. In all four cases, the forward propagating pulse with initial Gaussian profile undergoes a strong distortion inside the medium. For the instantaneous case, the modulation instability leads to a rapid anomalous spread of the pulse in both transverse and longitudinal directions, which demonstrates that phase changes of the beam in the transverse direction are sufficient to modulate the amplitude by the end of the medium. For short response time ( $\tau = 0.1$ ), not only does the profile of the forward propagating pulse undergoes a major distortion into an arch-like shape, but also the energy redistribution in both transverse and longitudinal directions becomes discontinuous. The intensity peaks appear at discrete spots, which can be readily seen in the 3-D plot of figure 4-3. A close look at forward propagating pulse shows that more high frequency components exist than in the case of instantaneous nonlinear PBG structure. As stated before, the Four Wave Mixing process in the Kerr medium is enhanced for small response times. In the instantaneous case, to generate MI, phase-match condition is required from the pump and probe, thus the generated frequency is strictly limited. But when the medium response time is taken into account, a Raman-like nonlinearity is developed for which self-phase-match is achieved, leading to a gain region outside the original sideband.

Previous studies show that the finite response time of Kerr effect alters the MI by lowering the gain and removing the gain cutoff frequency [45-46]. For short response time, the overall gain for small perturbations is only slightly decreased, but the whole gain region is widely extended, leading to a stronger break-up of the pulse. In the sub

frame for the backward propagating wave, we also observe an arch-like but weaker distortion than the forward propagating wave due to the limited passage in the nonlinear PBG structure. A rib structure is displayed which is also a characteristic of the longitudinal modulation instability.

As seen from Figure 4-2(c), Even for  $\tau = 1$ , the reshaping of both the forward and backward propagating waves into an arch pattern can still be observed. The distortion and rib structure are less obvious due to the weaker modulation instability.

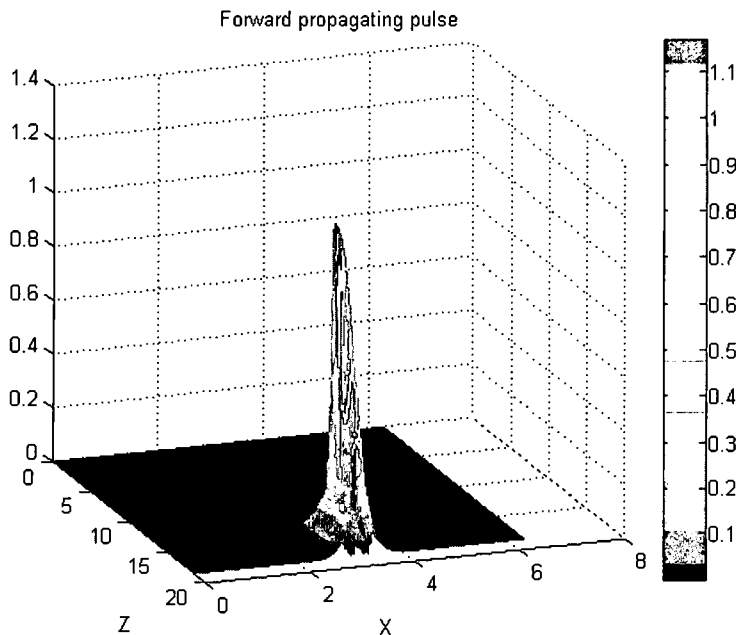


Figure 4-3 3-D structure of the forward propagating pulse.

As the response time largely increases as in Figure 4-2(d) ( $\tau = 4$ ), the pulse shape is only moderately distorted. The reason is that the overall gain that resulted from the modulation instability is greatly lowered by the long response time. The effect of the nonlinearity is abated. Also for the backward propagating pulse, the rib structure of the backward wave almost disappears, which is also a sign of the weak modulation instability.

## 4.2 PBG Optical Limiter

The ability of the non-instantaneous nonlinear PBG structure to break up a pulse makes itself a promising candidate for optical limiting. Since the energy of the incident pulse is spread longitudinally and transversely by the modulation instability, we place an aperture in the Fraunhofer regime after the PBG structure to further enhance the optical limiting as shown in Figure 4-4. The size of the aperture is set to be FWHM of the initial pulse, such that when the intensity is low, most part of the optical pulse is passed, and when the intensity gets undesirably high, a large portion of the spread optical is clipped. A probe is positioned behind the aperture to detect the transmitted energy.

Aperture placed behind the PBG structure in the far field

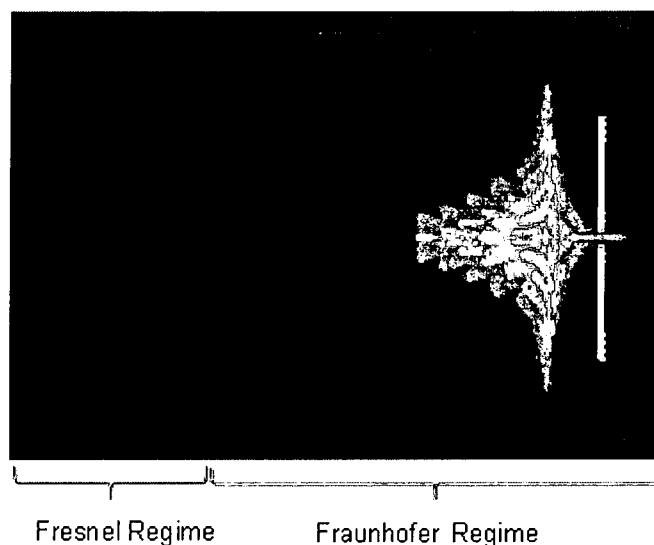


Figure 4-4 Aperture placed in the Fraunhofer regime to block out energy flow ( $A = 0.75, \tau = 1$ ). The Fresnel number is  $F = 10^7$ .

In order to evaluate the performance of the optical limiter , certain criteria need to be set up for comparison. Two figures of merit are proposed to categorize the performance of optical limiters. First, we define the transmission dynamic range (TDR) to be

$$TDR = \psi = \frac{T_{max}}{T_{min}} \quad (4-12)$$

Note that if  $T_{min}$  is zero, TDR is infinite for any nonzero  $T_{max}$ . Generally, TDR is more sensitive to the change in  $T_{max}$ . We define a second figure of merit related to the transmission cutoff (TCO) response band; it is defined by the intensity difference between the normalized 20% and 80% transmission points, i.e.

$$TCO = \frac{T_{80\%} - T_{20\%}}{T_{80\%} + T_{20\%}} \quad (4-13)$$

TCO shows how fast the transmission drops at the cut-off point. The smaller TCO is, the closer it approaches the ideal optical limiter.

Generally, an ideal optical limiter performance is approached as  $TDR \rightarrow \infty$  and  $TCO=0$ .

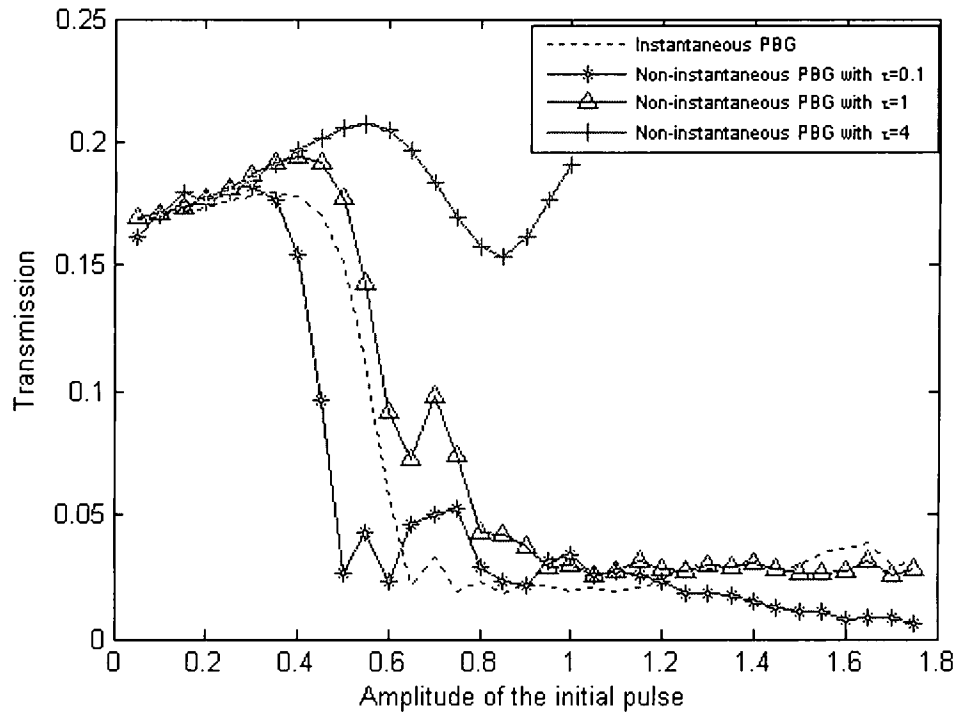


Figure 4-5 Normalized transmission curves for PBG structures with different response time.

Table 4-1 The figures of merit for instantaneous and non-instantaneous nonlinear media embedded in a PBG optical limiter.

Relaxation time of PBG	TDR	TCO
$\tau = 0$ (Instantaneous)	9.8004	0.209
$\tau = 0.1$	28.9355	0.190
$\tau = 1$	7.6128	0.465
$\tau = 4$	1.3556	N/A

Figure 4-5 summarizes the transmission characteristics for the non-instantaneous medium distributed in a PBG. We note that for small response time ( $\tau = 0.1$ ) the wave has a

higher  $T_{\max}$ , lower  $T_{\min}$  and decays faster than the instantaneous PBG. In terms of figures of merit, the optical limiting performance is improved in all aspects: higher TDR and lower TCO as shown in Table 1. Even for relatively long response time  $\tau = 1$ , the optical limiting properties are comparable to the instantaneous case. But for PBG structure with long response time ( $\tau = 4$ ), due to the weak modulation instability gain, the break-up of the pulse in the far field is dramatically suppressed, which reduces our optical limiting performance.

In this chapter, we presented a numerical model for counter-propagating waves in the one dimensional non-instantaneous nonlinear PBG structure. The case that the pulse is incident from one side of the PBG structure is especially stressed. The band-edge of the photonic crystal is manipulated to overlap with the center of the spectrum of the incident pulse to maximize the modulation instability. Our study shows that small finite response time of the Kerr effect ( $\tau = 0.1$ ) of the PBG can strengthen the spatio-temporal modulation instability of the medium, leading to a rapid spread of the pulse in the transverse direction and stronger temporal break-up of the pulse above threshold intensity. For relaxation times of order unity the performance of our optical limiter is not degraded over the instantaneous case. High frequency components are observed due to the extended “gain region” of the modulation instability, which leads to additional performance improvements for optical limiting applications. However, for long relaxation times, the nonlinear effect is weakened by lower gain of the modulation instability.

In Chapter 4.2 we applied the spatio-temporal modulation instability in non-instantaneous nonlinear PBG to design optical limiter. An aperture is placed in far-field

to filter high-intensity light before entering the detector. The performance of our design is evaluated in terms of dynamic range (TDO) and transmission cutoff (TCO). It is found that both figures of merit are improved in the case where the response time is short ( $\tau = 0.1$ ) compared to the pulse duration, which shows promising optical limiting characteristic. It is also found that material with long Kerr relaxational response times is not suitable for our design.

## Chapter V

### Conclusion

In this thesis, we presented the effect of non-instantaneous Kerr medium on the modulation instability and showed its affect on the propagation of both One-dimensional and multi-dimensional pulses. We showed that the finite response time of Kerr effect alters the MI by lowering the gain and removing the gain cutoff frequency. It is numerically demonstrated that a long relaxing time of the medium diminishes the nonlinear Kerr effect, resulting in a failure to maintain the shape of the solitary wave, which also leads to the arresting the collapse of Multi-dimensional pulses.

Based on the spatio-temporal modulation instability, we develop an optical limiter of One-Dimensional PBG structure with relaxational nonlinearity. The numerical model for counter-propagating waves in the one dimensional non-instantaneous nonlinear PBG structure is developed. The case that the pulse is incident from one side of the PBG structure is especially stressed. Our study shows that small finite response time of the Kerr effect of the PBG can strengthen the spatio-temporal modulation instability of the medium, leading to a rapid spread of the pulse in the transverse direction and stronger temporal break-up of the pulse above threshold intensity. For relaxation times of order unity the performance of our optical limiter is not degraded over the instantaneous case. An aperture is placed in far-field to filter high-intensity light before entering the detector. The performance of our design is evaluated in terms of dynamic range (TDO) and transmission cutoff (TCO). It is found that both figures of merit are improved in the case where the response time is short compared to the pulse duration, which shows promising



optical limiting characteristic. It is also found that material with long Kerr relaxational response times is not suitable for our design.

The optical limiter can be further improved by optimizing the parameters in the system. The other factors that we can modify to further improve the performance of the optical limiter include the aperture size, the length of the PBG structure, the complex third-order nonlinearity of the medium and the diffraction parameter  $F$ , beam focusing in the medium, and the beam shape. Based on earlier publications, longer pulses should possess better optical limiting performance.

## References

- [1] M. J. Miller, A. G. Mott and B. P. Ketchel, "General Optical Limiting Requirements," Proc. SPIE, **3472**, 24-29 (1998)
- [2] Charles W. Spangler, "Recent development in the design of organic materials for optical power limiting," J. Mater. Chem., **9**, 2013 – 2020 (1999)
- [3] T. Xia, D. J. Hagan, A. Dogariu, A. A. Said, and E. W. Van Stryland, "Optimization of optical limiting devices based on excited-state absorption," Appl. Opt. **36**, 4110-4122 (1997).
- [4] J. S. Shirk, R. G. S. Pong, F. J. Bartoli, and A. W. Snow, "Optical limiter using a lead phthalocyanine," Appl. Phys. Lett. **63**, 1880-1882 (1993).
- [5] J. Shirk, R. Pong, S. Flom, F. Bartoli, M. Boyle, and A. Snow, "Lead phthalocyanine reverse saturable absorption optical limiters," Pure Appl. Opt. **5**, 701-707 (1996).
- [6] P. Tran, "All-optical switching with a nonlinear chiral photonic bandgap structure," J. Opt. Soc. Am. B **16**, 70-73 (1999).
- [7] J. P. Dowling, M. Scalora, M. J. Bloemer and C. M. Bowden, "The photonic band edge laser: A new approach to gain enhancement," J. Appl. Phys. **75**, 1896-1899 (1994).
- [8] M. Scalora, J. P. Dowling, M. J. Bloemer and C. M. Bowden, "The photonic band edge optical diode," J. Appl. Phys. **76**, 2023-2026 (1994).
- [9] H-B. Lin, R. J. Tonucci, and A. J. Campillo, "Two-dimensional photonic bandgap optical limiter in the visible," Opt. Lett. **23**, 94-96 (1998).

- [10] M. Scalora, J.P. Dowling, C.M. Bowden and M. J. Bloemer," Optical limiting and switching of ultrashort pulses in nonlinear photonic band gap materials," *Phys. Rev. Lett.* **73**, 1368-1371 (1994).
- [11] Michael Scalora, Nadia Mattiucci, Giuseppe D'Aguanno, MariaCristina Larciprete, and Mark J. Bloemer, "Nonlinear pulse propagation in one-dimensional metal-dielectric multilayer stacks: Ultrawide bandwidth optical limiting," *Phys. Rev. E* **73**, 016603 (2006).
- [12] BoonYi Soon and Joseph W. Haus, "One-dimensional photonic crystal optical limiter," *Opt. Express* **11** 2007-2018 (2003).
- [13] T. Taniuti and H. Washimi, "Self-Trapping and Instability of Hydromagnetic Waves Along the Magnetic Field in a Cold Plasma," *Phys. Rev. Lett.* **21**, 209-212 (1968).
- [14] G. B. Whitham, "Non-linear dispersive waves," *Proc. R. Soc. London A* **283**, 238-261 (1965).
- [15] E. A. Kuznetsov, A. M. Rubenchik, and V. E. Zakharov, "Soliton stability in plasmas and hydrodynamics," *Phys. Rep.* **142**, 103-165 (1986).
- [16] A. M. Zheltikov, Let there be white light: supercontinuum generation by ultrashort laser pulses, *Physics-Uspekhi* **49**, 605-628 (2006).
- [17] W. -H. Chu, C. -C. Jeng, C. -H. Chen, Y. -H. Liu, and M. -F. Shih, "Induced spatiotemporal modulation instability in a noninstantaneous self-defocusing medium," *Opt. Lett.* **30**, 1846-1848 (2005)
- [18] D. Kip, M. Soljacic, M. Segev, E. Eugenieve, and D.Christodoulides, "Modulation Instability and Pattern Formation in Spatially Incoherent Light Beams," *Science* **290**, 495-498 (2000).

- [19] Yu. S. Kivshar and G. P. Agrawal, Optical solitons: From fibers to photonic crystals, (Academic Press, San Diego, CA, 2003).
- [20] R. W. Boyd, Nonlinear Optics, (Academic Press, San Diego, CA, 2003).
- [21] K. Tai, A. Hasegawa and A. Tomita, "Observation of modulational instability in optical fibers," Phys. Rev. Lett. **56**, 135-138 (1986).
- [22] G. P. Agrawal, "Modulation instability induced by cross-phase modulation," Phys. Rev. Lett. **59**, 880-883 (1987).
- [23] M. Mitchell, Z. Chen, M. F. Shih, and M. Segev, "Self-trapping of partially spatially incoherent light," Phys. Rev. Lett. **77**, 490-493 (1996).
- [24] C. Cambournac, H. Maillotte, E. Lantz, J. M. Dudley, and M. Chauvet, "Spatiotemporal behavior of periodic arrays of spatial solitons in a planar waveguide with relaxing Kerr nonlinearity," J. Opt. Soc. Am. B **19**, 574-585 (2002)
- [25] M. J. Potasek, "Modulation instability in an extended nonlinear Schroedinger equation," Opt. Lett **21**, 921 (1987).
- [26] J. W. Haus, B.Y. Soon, M. Scalora, M. Bloemer, C. Bowden, C. Sibilila and A. Zheltikov, "Spatio-temporal instabilities for counter-propagating waves in periodic media," Opt. Express **10**, 114-121 (2002).
- [27] B. Y. Soon, J. W. Haus, M. Scalora and C. Sibilila, "One-dimensional photonic crystal optical limiter," Opt. Express **11**, 2007-2018 (2003).
- [28] G. P. Agrawal, Nonlinear Fiber Optics, 3rd ed., (Academic Press, San Diego, CA, 2001).
- [29] T. R. Taha and M. J. Ablowitz, "Analytical and numerical aspects of certain nonlinear evolution- equation. 2. Numerical, nonlinear Schroedinger-equation," J.

Comput. Phys. **55**, 203-230 (1984).

[30] N. C. Kothari and S. C. Abbi, "Instability growth and filamentation of very intense laser beams in self-focusing media," Prog. Theor. Phys. **83**, 414-442 (1990).

[31] R. A. Fuerst, D.-M. Baboiu, B. Lawrence, W. E. Torruellas, G. I. Stegeman, S. Trillo, and S. Wabnitz, "Spatial modulational instability and multisolitonlike generation in a quadratically nonlinear medium," Phys. Rev. Lett. **78**, 2756-2759 (1997)

[32] M. Iturbe-Castillo, M. Torres-Cisneros, J. Sanchez-Mondragon, S. Chavez-Cerda, S. Stepanov, V. Vysloukh, and G. Torres-Cisneros, "Experimental evidence of modulation instability in a photorefractive Bi<sub>12</sub>TiO<sub>20</sub> crystal," Opt. Lett. **20**, 1853-1855 (1995).

[33] R. Malendevich, L. Jankovic, G. Stegeman, and J. S. Aitchison, "Spatial modulation instability in a Kerr slab waveguide," Opt. Lett. **26**, 1879-1881 (2001).

[34] R. Schiek, H. Fang, R. Malendevich, and G. I. Stegeman, "Measurement of Modulational Instability Gain of Second-Order Nonlinear Optical Eigenmodes in a One-Dimensional System," Phys. Rev. Lett. **86**, 4528-4531 (2001).

[35] Xiang Liu, K. Beckwitt, and F. Wise, "Transverse instability of optical spatiotemporal solitons in quadratic media," Phys. Rev. Lett. **85**, 1871-1874 (2000)

[36] X. D. Cao, G. P. Agrawal, and C. J. McKinstrie, "Self-focusing of chirped optical pulses in nonlinear dispersive media," Phys. Rev. A **49**, 4085-4092 (1994).

[37] Jinendra K. Ranka, Robert W. Schirmer, and Alexander L. Gaeta, "Self-focusing of chirped optical pulses in nonlinear dispersive media," Phys. Rev. Lett. **77**, 3783 - 3786 (1996)

[38] Y. Silberberg, "Collapse of optical pulses," Opt. Lett. **15**, 1282-1284 (1990);

- [39] J. H. Marburger and E. L. Dawes, "Dynamical Formation of a Small-Scale Filament," *Phys. Rev. Lett.* **21**, 556-558 (1968);
- [40] E. L. Dawes and J. H. Marburger, "Computer Studies in Self-Focusing" *Phys. Rev.* **179**, 862-868 (1969).
- [41] A. L. Dyshko, V. N. Lugovi, and A. M. Prokhorov, "Multifocus structure of a beam in a nonlinear medium," *Sov. Phys. JETP* **34**, 1235-1243 (1972).
- [42] B. J. Eggleton, C. M. deSterke, R. E. Slusher and J. E. Sipe, "Distributed feedback pulse generator based on nonlinear fiber grating," *Electron. Lett.* **32**, 2341-2342 (1996).
- [43] J. W. Haus, B. Y. Soon, M. Scalora, C. Sibilia, I. Mel'nikov, "Coupled-mode equations for Kerr media with periodically modulated linear and nonlinear coefficients," *J. Opt. Soc. Am. B* **19**, 2282-2291 (2002).
- [44] M. Mitchell, Z. Chen, M. F. Shih, and M. Segev, "Self-trapping of partially spatially incoherent light," *Phys. Rev. Lett.* **77**, 490-493 (1996).
- [45] Xue Liu, Joseph W. Haus and S.M. Shahriar, "Modulation instability for a relaxational Kerr medium," *Opt. Commun.* **281**, 2907-2912 (2008)
- [46] Ming-Feng Shih, Chien-Chung Jeng, Fan-Wen Sheu, and Chao-Yin Lin, "Spatiotemporal Optical Modulation Instability of Coherent Light in Noninstantaneous Nonlinear Media," *Phys. Rev. Lett.* **88**, 133902 (2002).

R0025939K